



ARTICLE

Prediction of Bandwidth of Metamaterial Antenna Using Pearson Kernel-Based Techniques

Sherly Alphonse^{1,*}, S. Abinaya¹ and Sourabh Paul²

¹School of Computer Science and Engineering, Vellore Institute of Technology, Chennai, 600127, India

²School of Electronics Engineering, Vellore Institute of Technology, Chennai, 600127, India

*Corresponding Author: Sherly Alphonse. Email: sherly.a@vit.ac.in

Received: 29 September 2023 Accepted: 11 December 2023 Published: 26 March 2024

ABSTRACT

The use of metamaterial enhances the performance of a specific class of antennas known as metamaterial antennas. The radiation cost and quality factor of the antenna are influenced by the size of the antenna. Metamaterial antennas allow for the circumvention of the bandwidth restriction for small antennas. Antenna parameters have recently been predicted using machine learning algorithms in existing literature. Machine learning can take the place of the manual process of experimenting to find the ideal simulated antenna parameters. The accuracy of the prediction will be primarily dependent on the model that is used. In this paper, a novel method for forecasting the bandwidth of the metamaterial antenna is proposed, based on using the Pearson Kernel as a standard kernel. Along with these new approaches, this paper suggests a unique hypersphere-based normalization to normalize the values of the dataset attributes and a dimensionality reduction method based on the Pearson kernel to reduce the dimension. A novel algorithm for optimizing the parameters of Convolutional Neural Network (CNN) based on improved Bat Algorithm-based Optimization with Pearson Mutation (BAO-PM) is also presented in this work. The prediction results of the proposed work are better when compared to the existing models in the literature.

KEYWORDS

Antenna; pearson; optimization; bandwidth; metamaterial

1 Introduction

Numerous studies in several disciplines have focused on metamaterials. Metamaterial antennas are another example of how metamaterials are used to enhance their performance. The loss of radiation and factor of quality of an electromagnetic antenna is influenced by its size. Compact antennas with increased gain and bandwidth can be produced using the metamaterial. Their electrical dimension should be as small as possible, and their directivity should be improved. The bandwidth constraints of small antennas can be overcome via metamaterial antennas. The influence of metamaterial on the antenna's parameters, such as its bandwidth and gain, is estimated using simulation software. With a supplement to simulation software, Machine Learning (ML) techniques might be employed to predict antenna properties. Using the best ML models, the models in [1,2] attempt to forecast the bandwidth and gain of the metamaterial antenna. Since metamaterial antenna has peculiar features,



it is being widely researched in the literature. These characteristics improve the capabilities of the source element and its industrial participation [3]. Computational electromagnetics is a branch of science and engineering that gives rise to metamaterial antennas. The foundation of computational electromagnetics is computation and technique optimization for antenna design. The purpose of this integration is to improve the metaheuristics that aid their search process, which eventually enhances the resilience, convergence rate, and solution quality. Additionally, there are several methods created to address the various optimization difficulties [4]. The capacity to establish an underlying link between the system input parameters and the envisioned results is the most significant advantage of ML-aided electromagnetics and as a result, the amount of computation required in experimental [5]. To address its significant complexity and computational cost, the use of ML in metamaterial antenna construction is a viable strategy [6]. A collaborative design for antenna selection was presented in [7]. Two deep learning models were also suggested, which will forecast the chosen antennas and predict hybrid beamformers. K-Nearest Neighbor (KNN) and Support Vector Machine (SVM) were used in a multiclass categorization of the Multiple-Input, Multiple-Output (MIMO) system-based antenna selection [8].

In [6], Artificial Neural Network (ANN) was used to identify the antennas having the lowest Signal-to-Noise Ratio (SNR) between users. For predicting a secure-based antenna on the wiretap medium, the authors of [9] combined naive Bayes and SVM into a hybrid machine learning algorithm. SVM was used in multiuser communication networks with multiple antennas. The SVM-based antenna scheduling system was proposed by the authors. The authors created a support vector regression model in [10] that was trained using information gathered to create the feed for a rectangular patch antenna, employing a microwave simulator. The foundation of ensemble ML is the combination of many ML techniques such as KNN, SVM, and ANN [11]. Using the average of the output readings to estimate an output is the fundamental idea behind ensemble learning which is used in certain approaches. Even though several approaches exist in the literature, there is a need for better normalization techniques, dimension reduction techniques, and optimization techniques for choosing the parameters of the neural networks used in the classification. This research will result in the following goals:

- Founding a novel approach based on applying Pearson Kernel as the universal kernel for finding the bandwidth of the metamaterial antenna.
- Founding a novel hypersphere-based normalization to normalize the values of the dataset attributes.
- Developing a novel dimensionality reduction technique based on Pearson kernel for reducing the dimensions of the attributes.
- Developing a Pearson-kernel-based bat optimization algorithm for the optimization of the parameters of Convolutional Neural Network (CNN).
- Evaluating how well the suggested model predicts the metamaterial antenna's bandwidth in comparison to the most recent ML models.

Small antenna bandwidth restrictions can be overcome with metamaterial antennas. Recently, ML algorithms have been used in the literature to predict antenna parameters. To determine the optimal simulated antenna parameters, manual experimentation can be replaced by machine learning. The model that is employed will have the biggest impact on the accuracy of the predictions. This paper presents a novel approach based on the Pearson kernel as a standard kernel for forecasting the bandwidth of the metamaterial antenna. This paper proposes a novel hypersphere-based normalization technique to normalize the values of the dataset attributes along with a dimensionality reduction

method based on the Pearson kernel. This work also presents an algorithm for CNN parameter optimization based on improved Bat Algorithm-based Optimization with Pearson Mutation (BAO-PM). The remainder of the paper is divided into the following sections. The associated work is defined in Section 2. The proposed work is defined in Section 3. The results are reported in Section 4, and the conclusion is covered in Section 5.

2 Related Work

It was suggested in [12] to optimize the Frequency Selective Surface (FSS)-based filtering antenna with a lesser computational complexity. Signals at a certain frequency are enhanced and filtered by the Filtenna. The complex relationships and large number of factors that impact scattering reactions make it difficult to construct Filtenna FSS components. The authors develop a precise representation of unit cell activity using customized multilayered perceptron (M2LP), a deep learning technique that results in enhanced optimization. To speed up antenna tuning, Pietrenko-Dabrowska et al. [13,14] proposed a technique that restricts antenna response intensity upgrades. The predicted antenna properties change when traveling across the one-dimensional linear sub-space represented by these axes. Local optimization is used to reduce the computational expenses for full-wave Expectation-Maximization (EM) computations employed in the optimization of antenna. The outcomes demonstrate a 70% acceleration over benchmark methods without compromising quality. Many antenna layouts and faster variants of trusted sector procedures are used to test the strategy.

Reflectarray (RA) problems with design have been discussed in [15]. RAs have benefits over conventional antenna arrays but have limited losses and bandwidth. For precise transistor dispersion and noise factor simulation using ANN, a Fully Adaptable Regression Method (FARM) was put into practice [16]. To correlate inputs and network design, a tree Parzen predictor recognizes all elements of the network and handles tasks of processing in the FARM approach. When the original design is close to the optimum, gradient-based EM-driven circuit closure procedures perform effectively. A subpar local optimum may be reached by the method of search if the original layout is not ideal. The computational expense of simulation-based refinement is high. A novel approach to parameter tweaking via variable-resolution EM systems was suggested by some studies [17]. Table 1 gives a short survey of the existing optimization techniques.

Table 1: Comparison of different optimization techniques

Existing approaches	Techniques	Potency	Inadequacy	Applications
Grey wolf optimizer (GWO) algorithm [18]	It imitates the social structure and authority of grey wolves in their hunting activity. Individuals in the pack follow the three leaders when they hunt.	The distinction between mining and investigating is appealing and the search accuracy is great.	Performance degrades due to an excessive amount of variables in the optimization process.	Clustering process, designing of antenna, robotics and pathfinding.

(Continued)

Table 1 (continued)

Existing approaches	Techniques	Potency	Inadequacy	Applications
Sine cosine algorithm (SCA) [19]	The direction of movement and length are tracked, the impact of the end point is either over- or under-emphasized, or the sine and cosine elements are alternated between a series of random variables.	It uses memory effectively, has a significant rate of exploitation, and converges quickly.	Minimal exploratory level, performance deteriorates when there are several optimal local remedies available, and the search procedure is based on just the best solution.	Signal processing, filter architecture, predicting solar radiation, and designing antenna.
Particle swarm optimization (PSO) [20]	It draws inspiration from the conversations and dynamics of flocks of birds and fish.	Excellent cooperative model with stable convergence and ease of application.	There is a slow convergence, a large computing cost, and difficulty in determining the initial parameters.	Gene clustering, vehicle routing, reducing dimensionality and antenna design.
Whale optimization algorithm (WOA) [21]	This method is inspired by the bubble-net aging pattern of humpback whales.	The search space has a vast exploration scope and is easy to apply.	There is a large computational cost, a chance of stalling in local optimal values, and a slow rate of convergence.	Design of antenna, precise laser sensor control systems, planning tasks, optimization of routes, and drift voltage minimization.
Genetic algorithm (GA) [22]	The biological evolution theory which holds the survival of the fittest is the foundation for this algorithm. Initializing, parent choice, crossover over, and mutagenesis are the stages of GA.	Noisy effects are simply handled which are devoid of gradients, and straightforward to implement.	The lack of appropriate complexity scaling makes it difficult to adjust the parameters, the convergence happens prematurely, and the rate of convergence is slow.	Engineering applications, robot route establishing and design of filter and antenna.

The dimensional problem, which affects conventional metamodelling techniques, prevents them from functioning while dealing with nonlinear antenna features over an extensive spectrum of network parameters. This problem can be solved by performance-driven design systems, which creates models based on performance of antenna data instead of geometric parameters [23,24]. The antenna structure in the work by the author in [25] has twelve unit Meta Surface cells. To maximize performance, the antenna structure is simulated using the Computer Simulation Technology Microwave Studio (CST MWS) package, which includes all design methodologies. The High-Frequency Structure Simulator (HFSS) software package is utilized to validate the ideal antenna design through numerical testing. This gain bandwidth product of the system was excellent. Through metasurface (MTS), the antenna bandwidth is enhanced. CNN is used to study the design process parametrically. As a result, the CNN is an effective tool for parameter prediction. The proposed work can also be applied to such antenna structures for improved performance. In the proposed work, a unique method for predicting the metamaterial antenna's bandwidth is developed using the Pearson Kernel (PK) as the global kernel. To normalize the values of the properties of the dataset, a unique hypersphere-based normalization is also developed. It normalizes and eliminates data overlapping by mapping the characteristics onto the surface of a hypersphere. The Pearson kernel is proposed as a novel kernel that achieves good performance over all the existing kernels in literature. It is used in kernel-based Principal Component Analysis (PCA) as Pearson Kernel-based Supervised PCA (PKSPCA) in the proposed technique. Then a Pearson mutation-based Bat optimization algorithm is also proposed for optimizing the weights of CNN that helps in achieving good accuracy compared to existing techniques. The proposed optimization algorithm uses Pearson mutation which helps in faster convergence. The results signify the improved act of the proposed technique.

3 Proposed Methodology

Low-profile microstrip antennas are used in high-performance aircraft, spacecraft, satellite, and missile applications where aerodynamic profile, size, weight, performance, and ease of installation are constraints. Wireless connections and mobile communication are examples of civilian applications. Particular arrangements of unit cells with unusual electrical characteristics are known as metamaterials. These materials have characteristics not found in the natural world. The magnetic permeability and electrical permittivity are negatives as a result of these dispositions. As a result, there is negative refraction, which alters the expected behavior of electromagnetic radiation. A dataset having results of electromagnetic simulations of metamaterial antennas is used in the proposed work. Fig. 1 displays the general layout of the proposed technique. The method begins by putting together a dataset for the metamaterial antenna and using simulation tools to capture the design parameters, as seen in the image. Before training the recommended deep network, preprocessing is an essential step that must be carried out because the dataset may contain some records of the design parameters with incorrect or null values. After preprocessing is complete, the dataset is divided into the train, validation, and test sets to be used to train the deep network. The CNN can be used to predict the ideal values of antenna parameters once it has been trained; in our case, it is utilized to forecast the bandwidth of the metamaterial antenna. The unique properties of the metamaterial allow antenna designers to create antennas with unique features, in contrast to the conventional material used in antenna design. In addition to applying one or more metamaterial layers to the antenna substrate, specific design parameters can be set to enhance the performance of antennas that use metamaterial. A Split Ring Resonator (SRR) unit cell for a metamaterial antenna is shown in Fig. 2 and is defined by the dataset used in this study. SRR is represented by two rings with a space in between. SRR is significant because it allows the bandwidth of the metamaterial antenna and mutual coupling to be reduced. The y-axis

represents the Perfect Magnetic Conductor (PMC) of the metamaterial antenna on the radiation box's surface.

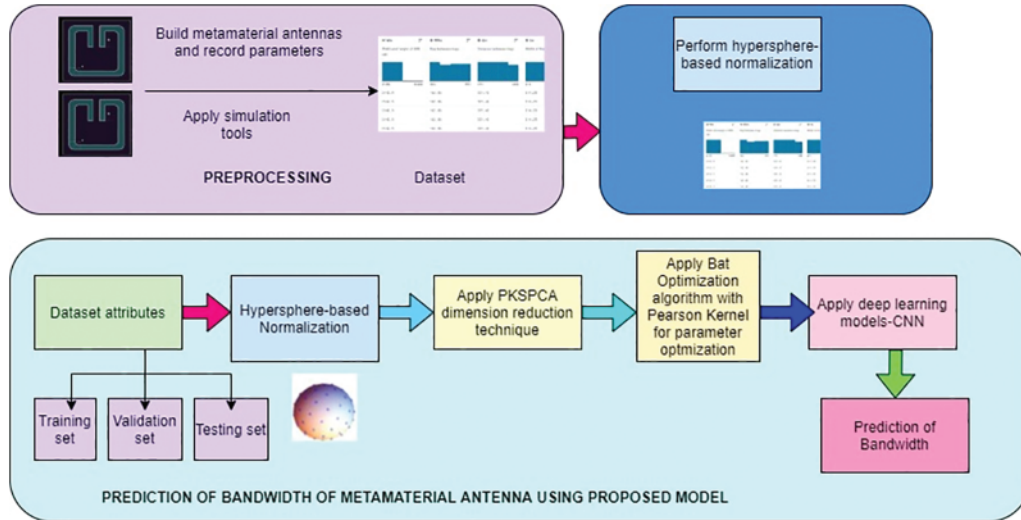


Figure 1: Overall architecture for prediction of bandwidth

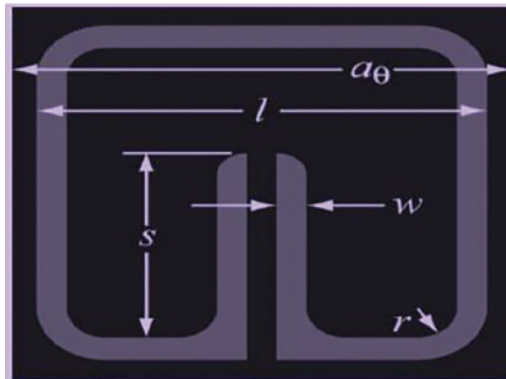


Figure 2: Shape of the split ring resonator. The parameters of the lattice in-plane are $a_\theta = a_z = 10/3$ mm. The ring has a square shape, with a trace width w of 0.2 mm and an edge length l of 3 mm. The substrate is Duroid 5870, which has a thickness of 381 μm and a loss tangent of $t_d = 0.0012$ at 10 GHz ($\epsilon = 2.33$). The thickness of the Cu film used to pattern the SRRs is 17 μm . The length of the split s and the radius of the corners r are the two geometric parameters that are adjusted to adjust the split ring resonator. The imaginary parts of ϵ_z and μ_r , respectively, yielded values of 0.002 and 0.006. The inner cylinder is 1 and the outer cylinder is 10

3.1 Dataset

The dataset used in this study contains 10 attributes that are used to define the design parameters of metamaterial antenna. On Kaggle [26] (Metamaterial Antennas | Kaggle), this dataset is accessible in tabular form with predefined rows and columns. This dataset contains 572 rows (records), 10 columns (parameters), and the following values: antenna gain, voltage standing wave ratio, return loss, gap amid

rings, width of rings, distance amid rings, bandwidth, antenna patch, and distance among split-ring resonator cells in the array. Table 2 displays these parameters along with the accompanying symbols. In this study, nine of these factors are used to forecast the bandwidth of a metamaterial antenna. The correlation matrix, which determines the correlation between the attributes of the dataset for study, is displayed in Fig. 3. Fig. 3 clearly shows the substantial correlation between bandwidth and both Ya and Xa. Less strongly correlated are the bandwidth, Wm, and Tm.

Table 2: The parameters in the dataset

Sl. No.	Attributes	Dataset
1	Wm	Dimensions of the resonator with split-ring
2	W0m	The gaps in the ring
3	Dm	Distance of ring
4	Gain	Antenna gain
5	Xa	Antenna patch and array distance
6	Tm	Ring width
7	Ya	Cell distance in the split ring resonator
8	VSWR	Voltage wave ratio
9	Bandwidth	Bandwidth of antenna
10	S11	Loss

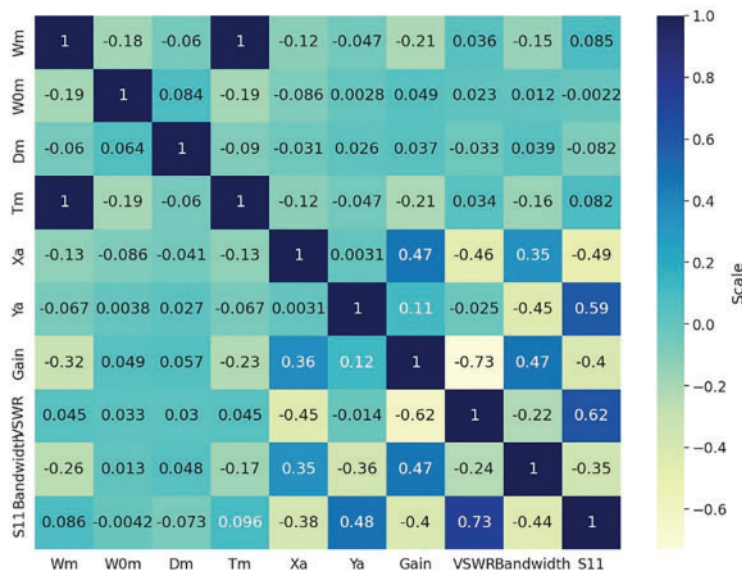


Figure 3: Correlation measure of the design parameters

3.2 Data Preprocessing

A set of preparation chores must be completed before using machine learning techniques on the provided dataset. Additionally, the efficacy of machine learning algorithms is typically impacted by

the range of the features of the dataset. Scaling and normalizing all of the characteristics of the dataset is the second step in the preparation phase. Because these features fall within the same range of values, machine learning may treat them similarly. This study uses hypersphere-based normalization to scale the features and bring them within the range of the hypersphere.

3.3 Novel Hypersphere-Based Normalization Method

The proposed study uses the hypersphere-based normalization technique, which, unlike other normalization techniques, achieves effective normalization without overlapping. It also enhances the numerical characteristics of the kernel matrix by reducing the effect of other transformation variables on the features. Since the distances among the features projected onto the Hypersphere are relative to their original distances, these points are mapped to be scattered over the hypersphere without any overlaps. As a result, the proposed study uses the hypersphere-based normalization technique, which, unlike other normalization techniques, achieves effective normalization without overlapping.

The inner products between the data points have to be smooth to be mapped onto the Hypersphere. According to Boumal et al. [27], the smooth inner product is computed using the Conjugate Gradient solver of the Matlab Toolbox for Optimization on Manifolds (MANOPT) tool. By making the feature space a Riemannian manifold, the optimization problem is solved. Fig. 4 explains the algorithm used for hypersphere-based normalization of the features in the dataset. The algorithm is said to be complete when the inner product variable is smooth or when the specified tolerance criterion is satisfied. After initially traveling in the direction of $d_0 = \Delta a_0$, the algorithm moves in the direction of t_m . The globally convergent Conjugate Gradient technique is used to design the algorithm for changing the feature space to build a smooth inner product. When the inner product variable is nearly uniform or the stated tolerance condition is met, the algorithm is considered to have finished. The smoothing of the inner products scatters the properties of the new dataset over the closed hypersphere surface. The properties of the normalized attributes in the dataset are contained within a predetermined range. The normalized attributes are then made available for CNN classification. The next section explains the novel dimensionality reduction technique used for reducing the dimensions of the features.

Algorithm	Hypersphere-based normalization
Input	: Non-scaled attributes of the dataset, A_m .
Output	: Normalized attributes which pacifies the conditions to be distributed on a Hypersphere.
Parameters:	<p>A_m - Dataset's attributes</p> <p>ΔA_m - Steepest direction.</p> <p>$f(A_m)$ - Function for conviving inner product among the dataset's attributes.</p> <p>d_m - Conjugate direction.</p> <p>d_0 - Preliminary search direction.</p> <p>β_m - Parameter accountable for the direction reset.</p> <p>α_m - Adaptive step length</p> <p>While inner product is not uniform in the attribute space of the dataset</p> <ul style="list-style-type: none"> • Calculate $\Delta A_m = -(\nabla_A f(A_m))$. • Update $t_m = -(\nabla_x f(A_m)) + \beta_m t_{m-1}$. • Estimate $\beta_m = -\frac{\Delta A_m^T (\Delta A_m - \Delta A_{m-1})}{t_{m-1}^T (\Delta A_m - \Delta A_{m-1})}$. • Complete a line search, then optimize and compute $\alpha_m = \min_{\alpha > 0} f(A_m + \alpha t_m)$. • Re-calculate each attribute A_m using $A_{m+1} = A_m + \alpha_m t_m$.
End.	

Figure 4: Correlation measure of the design parameters

3.4 The Proposed Pearson Kernel-Based Dimensionality Reduction Technique

The properties of the compact dataset are represented using Pearson Kernel-Based Supervised Principal Component Analysis (PKSPCA), which eliminates both redundant features including noise, and yields the greatest performance. The proposed innovative PKSPCA assists in cutting down on calculation time significantly [28]. A new Pearson kernel, which aids in achieving a superior act compared to the other kernels such as linear, polynomial, and Gaussian, is projected in the proposed approach. Here, M is the space for the answer variable and N is the attribute space:

$$M = [m_1, m_2 \dots m_N]^T \tag{1}$$

$$N = [n_1, n_2 \dots n_N]^T \tag{2}$$

$$D = \{(m_1, n_1), (m_2, n_2), (m_3, n_3) \dots (m_4, n_4)\} \tag{3}$$

If F and G are discrete Reproducing Kernel Hilbert Spaces (RKHS), which comprise all endlessly limited real-valued functions of M and N , the empirical Hilbert Schmidt independence criterion (HSIC) can be determined as follows:

$$HSIC_{em}(D, F, G) = (A - 1)_2 Tr(KSLS) \tag{4}$$

$Tr(\bullet)$ stands for the trace of a square matrix, while K and L are the kernel matrices of F and G based on the kernel functions $k()$ and $l()$, respectively.

$$K_{ij} = k(x_i, x_j) \quad \text{and} \quad L_{ij} = l(y_i, y_j) \tag{5}$$

S is referred to as the mean subtraction matrix and has the formula $S = I - \frac{ee^T}{A}$, where I is the identity matrix with order A and e denotes a column vector of order A . The dependency between $U^T X$ and Y are being maximized in the subspace $U^T X$. The HSIC measures the interdependence between X and Y and is used to maximize $Tr(KSLS)$ to solve the optimization problem. Here,

$$K = (U^T X)^T (U^T X) \tag{6}$$

$$U^T U = I \tag{7}$$

The optimization problem now becomes as $\max_U Tr(U^T X S L S X^T U)$ and $U^T U = I$. In the PKSPCA X is substituted by $\Phi(X)$ and $U = \Phi(X)\alpha$. Therefore, the objective function is given as follows:

$$\max_U Tr(\alpha^T K^* S L S K^* \alpha) \tag{8}$$

where K^* and L are the proposed Pearson general kernel-generated kernel matrices of order N . The proposed Pearson function is employed as the universal Pearson kernel [11]. As a result, the Pearson kernel can be used across all datasets rather than alternative state-of-the-art kernels being tested. The time required for choosing the kernels and performing the computations is decreased by the proposed PKSPCA.

$$\frac{1}{\left[1 + \left(\sqrt{\|x_{ki} - x_{kj}\|^2} \sqrt{2\left(\frac{1}{\omega}\right) - 1/\sigma} \right)^2 \right]^\omega} \tag{9}$$

The solution to the optimization issue is the B eigenvectors of $(K^* S L S K^*, K^*)$ based on the first B eigenvalues. The kernel matrices K^* and L concerning X and Y are computed using a Pearson kernel,

where k is the function of the kernel. Analytically expressing the response to the objective function results in F of order BA , the newly created low-dimensional space. As a result, the following may be said about the low dimensional features (DF), that the PKSPCA gathered from the samples:

$$DF = \hat{\alpha}^T K^* \quad (10)$$

The CNN then predicts the bandwidth using a lower dimensional attribute space.

3.5 Classification Using Optimized CNN with Pearson Mutation-Based Bat Optimization

CNN employs a non-linear function called the Fully Connected layer [29]. The model uses the Softmax approach to predict the bandwidth over numerous epochs. The Rectified Linear Activation Unit (ReLU) compares the input with the value 0 as part of its operation. The dimension of the feature maps is decreased by pooling layers. The streamlined features in the feature map are produced by the pooling layer. The accuracy discovered via CNN is employed as the fitness function when employing the Bat algorithm-based optimization [30] for tuning the CNN parameters. Fig. 5 depicts the algorithm used to identify the optimized values for parameters. The best value, in contrast to other values, necessitates the mutation operator moving forward. The various parameters used in CNN are given in Tables 3 and 4.

Table 3: The parameters used for training in CNN

Parameters	Value
Number of epochs for optimum CNN	20
Number of epochs for training	60
Rate of dropout	0.6
Size of Minibatch	256
Learning rate in initial stages	0.002

Table 4: Parameter values of CNN

Parameters	Value
Least count of layers	3
Highest count of layers	12
Least count of filters	16
Highest count of filters	256
Least size of convolution kernel	2
Highest size of convolution kernel	12
Least size of kernel in layer for pooling	2
Highest size of kernel in layer for pooling	8
Least size of stride in pooling layer	2
Highest size of stride in pooling layer	8
Least size of neurons	12
Highest size of neurons	1024

Algorithm 1 Parameter optimization using the Bat method and Pearson Mutation

Procedure BAO_PM (α, λ)

Input: A series of values for parameters of CNN

Output: Best values for parameters of CNN

Parameters:

α —Range of values of α for parameters of CNN

$updated_ \alpha$ —Optimized value for parameters of CNN

α_{i-1} th value of α for parameters of CNN

CNN accuracy— CNN accuracy using α_i set parameters of CNN

CNN accuracy is evaluated as this algorithm's fitness parameter and goal function.

1. Initialize the values of α ;
 2. Assess the initial population;
 3. **While** the end condition is not reached;
 4. Generate new solutions by changing α_i ;
 5. Compute Pearson(b_1, b_j) =
$$\frac{1}{1 + \left(\frac{2 \sqrt{\|b_1 - b_j\|^2 \sqrt{2^{(1/\omega)} - 1}}}{\sigma} \right)^{2/\omega}}$$
 6. Estimate $W_j = (\sum_{i=1}^N R_{ij}) / N$;
 7. Estimate $V_j = R_{ij} + W_j \cdot \text{Pearson}(\omega, \sigma)$;
 8. Apprise α_i using Pearson Mutation (PM);
 9. Get CNN accuracy;
 10. **If** CNN accuracy > best_accuracy;
 11. Customary updated_ $\alpha = \alpha_i$;
 12. Customary best_accuracy = CNN accuracy;
 13. Decide the best_accuracy as global optimal;
 14. Apprise α_i ;
 15. **End**;
 16. **End While**;
 17. Store new_ α ;
 18. Allocate the values of α ;
 19. **Return** new optimized values of α ;
 20. **End Procedure**.
-

Figure 5: The algorithm for BAO_PM

4 Results and Discussion

To illustrate the performance of the suggested methodology, the dataset is divided into three subsets: the train, validation, and test sets. The training subset has a ratio of 80% to 20%, while the testing subset is 20% smaller. The training subset is 25% smaller than the validation subset. The proposed deep network is trained by setting the network parameters to random values at the beginning. After that, using the guided BAO-PM, some iterations are performed to find the best values for these parameters. During training, the network seeks to develop its antenna bandwidth prediction skills. The performance of the trained network is assessed using the Mean Square Error (MSE) metric. Here is the formula for this measure.

$$MSE = \frac{1}{n} \sum_{i=1}^n (Y_i - Y_i^*)^2 \tag{11}$$

where n is the total number of samples in the evaluation set, and Y_i and Y_i^* stand for the antenna's expected bandwidth and actual values, respectively.

Table 5 only displays the best results from testing different kernels in the suggested work for dimension reduction. The collection of values $\{2^{10}, 2^9, \dots, 2^{-9}, 2^{-10}\}$ is used to select the Radial Basis Function (RBF) kernel parameter σ . The grid search method is coupled with cross-validation on the samples used as the training set. Then, for the Pearson kernel in the proposed study, σ is selected from the set $\{2^{10}, 2^9, \dots, 2^{-9}, 2^{-10}\}$ and ω is selected from the set $\{2^0, 2^1, \dots, 2^{10}\}$. The set of parameters that maximizes classification accuracy is the ideal set for the test set. Once the deep network has been

trained, the test set is utilized to evaluate the robustness of the trained model [24,25]. The results signify that the Pearson kernel achieves higher accuracy when used for dimension reduction compared to the other kernels. The quantile-quantile (QQ) plot are displayed in Fig. 6. The diagonal line connecting the expected and actual residuals is fit by the distribution of the QQ plot's points, as seen in the image. The predicted and actual values of the parameters are mapped out in a QQ plot. The mapping in this figure roughly fits a straight line, highlighting the efficiency of the suggested algorithm. This fitting verifies how well the proposed model predicts the bandwidth. The residuals and homoscedasticity of the prediction outcomes using the suggested Pearson kernel-based model are shown in the plots in Figs. 7 and 8. The residual error values are near zero, as shown in the figure, confirming the efficacy of the suggested technique. A homoscedasticity plot can also help determine whether the independent variables have the same error term, which can be determined from the plot values. The Receiver Operating Characteristics (ROC) of the suggested approach are also displayed in the plots of Fig. 9. These principles highlight how efficient the suggested strategy is.

Table 5: Comparison of categorization accuracy found in the literature using different kernels

Datasets	Proposed approach using various kernels			
	Linear	Polynomial	RBF	Pearson kernel
Metamaterial antenna	96.9	93.9	95.5	99.7

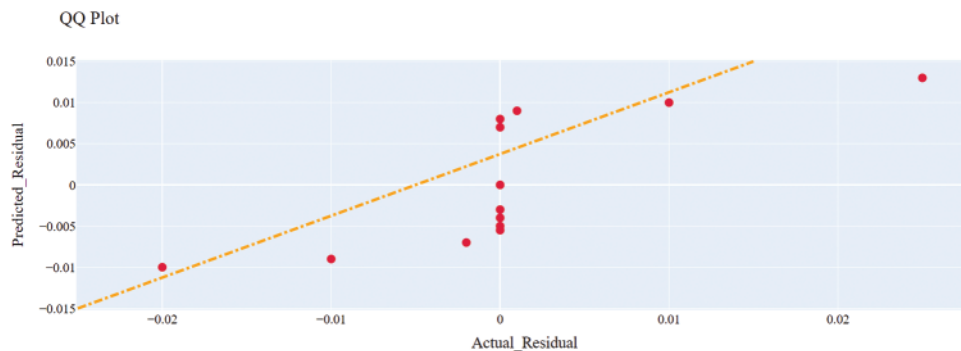


Figure 6: QQ plot

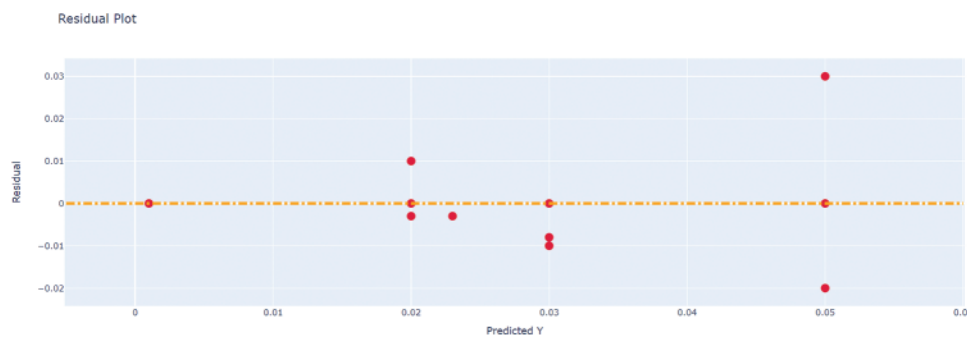


Figure 7: Residual plot

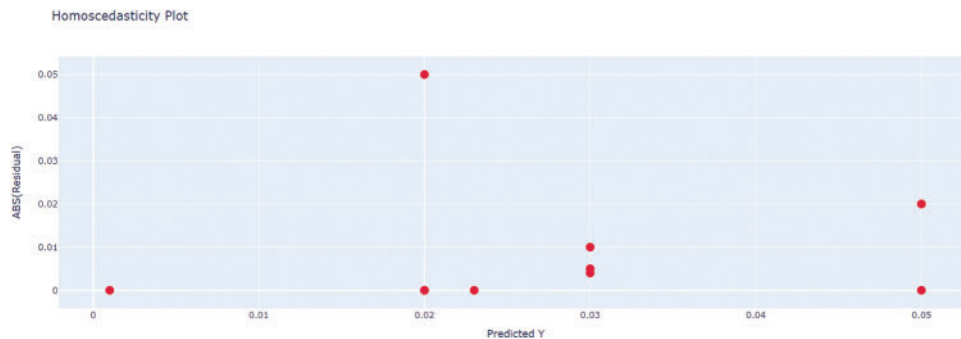


Figure 8: Homoscedasticity plot

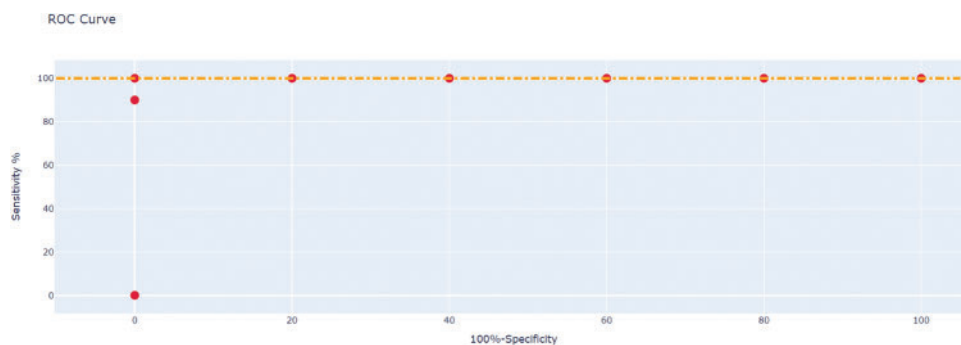


Figure 9: ROC curve

The evaluation of the model using different classifiers based on the metamaterial antenna test set is shown in [Table 6](#). The findings obtained by the suggested model are represented in [Table 6](#). These results are superior to those of the three rival methodologies Multilayer Perceptron (MLP), K-Nearest Neighbor (KNN), and Long Short Term Memory (LSTM) [30–38]. The table includes a list of additional evaluation criteria, the measured values of which are significantly higher than what the other models achieve. These measurements include the Mean Absolute Percentage Error (MAPE), Mean Absolute Error (MAE), Mean Bias Error (MBE), Coefficient of Determination (R2), Determine Agreement (WI), Nash Sutcliffe Efficiency (NSE), the Relative Root Mean Square Error (RRMSE), Pearson’s correlation coefficient (R), and the Root Mean Square Error (RMSE). [Table 7](#) also contains the descriptive statistics of the recommended strategy over 20 runs.

Table 6: Comparison of proposed model with other classifiers

	MLP	KNN	LSTM	CNN
R	1.00	1.00	1.00	1.00
MAE	0.06	0.03	0.03	0.01
RMSE	0.06	0.04	0.03	0.01
MBE	−0.03	0.01	0.01	0.01
RRMSE	8.73	4.71	11.59	0.53

(Continued)

Table 6 (continued)

	MLP	KNN	LSTM	CNN
R2	0.99	1.00	1.00	1.00
WI	0.88	0.95	0.97	1.00
NSE	0.95	0.99	1.00	1.00

Table 7: The descriptive statistics of the proposed model and existing models

Descriptive statistics	MLP	KNN	LSTM	Proposed model
Count of values	15	15	15	15
Least	0.04	0.03	0.03	0.01
25% percentile	0.06	0.04	0.03	0.01
Median	0.06	0.04	0.03	0.01
75% percentile	0.06	0.04	0.03	0.01
Highest	0.09	0.05	0.04	0.01
Series	0.06	0.03	0.02	0.01
10% percentile	0.05	0.03	0.03	0.01
90% percentile	0.08	0.04	0.03	0.01
95% confidence interval of median	0.01	0.01	0.01	0.01
Definite confidence level	1.00	1.00	1.00	1.00
Minor confidence limit	0.06	0.04	0.03	0.01
Higher confidence limit	0.06	0.04	0.03	0.01
Mean	0.06	0.04	0.03	0.01
Std. deviation	0.02	0.01	0.01	0.01
Std. error of mean	0.01	0.01	0.01	0.01
Lesser 95% confidence interval of mean	0.06	0.04	0.03	0.01
Higher 95% confidence interval of mean	0.07	0.04	0.03	0.01
Coefficient of variation	0.20%	0.13%	0.12%	0.01%
Geometric mean	0.06	0.04	0.03	0.01
Geometric standard deviation factor	1.21	1.13	1.11	1.02

When compared to the similar values estimated from the outcomes obtained by the other ways, as indicated in the table, the calculated values of these statistics utilizing the suggested approach are reassuring. These numbers represent the effectiveness and superiority of the suggested model in estimating the bandwidth of the metamaterial antenna. The suggested strategy and the other approaches are statistically significant, as in the table. Here an additional test is done using the two-tailed t -test between each of the two algorithms to unequivocally demonstrate the superiority of the suggested method. [Table 8](#) presents the test results for 21 samples at the 0.05 significance level. If the p -value of less than 0.05 indicates that the algorithm is significant. The measured p -value in [Table 8](#) satisfies the condition and indicates their significance. Nonetheless, the suggested method was able to attain the least amount of difference between the tested models, demonstrating the superiority of the suggested

algorithm and bolstering its increased statistical significance. Figs. 10a–10c illustrate the RMSE plots for different optimization algorithms, dimension reduction techniques (Principal Component Analysis (PCA), Linear Discriminant Analysis (LDA), Fisher Linear Discriminant Analysis (FLDA)), and normalization techniques [39] used in the proposed work. The RMSE plots show improved performance for the proposed BAO-PM, PKSPCA, and hypersphere-based normalization techniques in the proposed work. When compared to the other approaches, the suggested strategy yields the lowest discrepancy values over the test set, as the table illustrates. The remaining results, which are shown in the figures and tables, demonstrate the stability of the suggested method for estimating the bandwidth. Among the corresponding predictions made using the other feature selection algorithms, most of the predicted values in this figure have the lowest RMSE values. The majority of the obtained RMSE values fall between (0.002) to (0.004), surpassing the results attained by the other algorithms.

Table 8: The two tailed t -test using different optimization algorithms in the proposed method

	SCA-CNN	GWO-CNN	WOA-CNN	PSO-CNN	BAO-PM-CNN
Theoretical mean	0	0	0	0	0
Actual mean	0.000002848	0.00003961	2.957E-07	6.805E-07	2.805E-100
Count of values	21	21	21	21	21
<i>Single sample t test</i>					
t-distribution, degrees of freedom (df)	t = 14.74, df = 20	t = 42.89, df = 20	t = 20.20, df = 20	t = 41.78, df = 20	t = 24.30, df = 20
p -value (two tailed)	<0.0001	<0.0001	<0.0001	<0.0001	<0.0001
Substantial (alpha = 0.05) ?	Yes	Yes	Yes	Yes	Yes
Discrepancy	0.000002456	0.00003234	2.834E-07	6.785E-07	2.785E-100
Standard deviation of discrepancy	9.451E-07	0.000003982	6.567E-08	7.678E-08	5.56E-101
Standard error of the Mean of discrepancy	2.067E-07	8.378E-07	1.456E-08	1.677E-08	1.188E-101
95% confidence interval	2.5E-6 to 3.4E-6	3.3E-5 to 3.7E-5	2.6E-7 to 3.2E-7	6.6E-7 to 7.3E-7	2.7E-100 to 3.20E-100
R squared (partial eta squared)	0.9178	0.956	0.9356	0.9789	0.9345

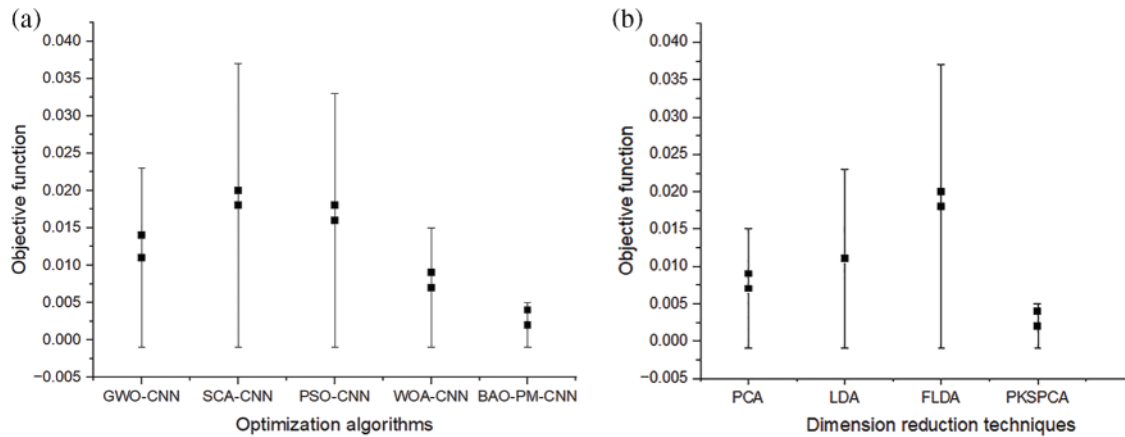


Figure 10: (Continued)

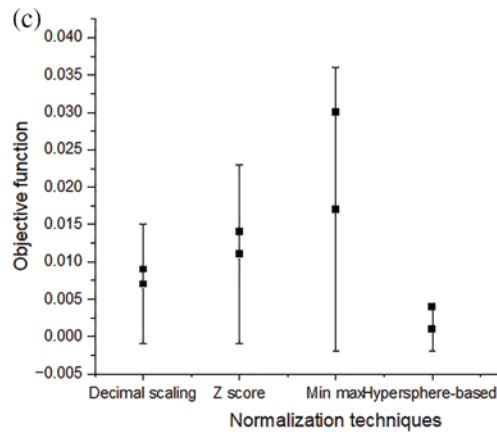


Figure 10: (a) RMSE plot of different optimization algorithms in the proposed model. (b) RMSE plot of different dimension reduction techniques in the proposed model. (c) RMSE plot of different normalization techniques in the proposed model

5 Conclusion

In this research, a unique CNN-based approach is presented for forecasting the parameters of metamaterial antenna. Based on a set of design criteria, the suggested approach can precisely estimate the bandwidth of metamaterial antennas. The Pearson Kernel shows superior results when compared to the other kernels while it is used for dimension reduction in the proposed work as seen in the results. The actual and anticipated bandwidths were examined in this investigation to emphasize and confirm the robustness of the suggested strategy. To demonstrate the superiority of the suggested algorithm, the results produced were also compared to those of other optimization algorithms. Prospects for this research in the future include evaluating the suggested algorithm in different antenna structures [25] and other optimization scenarios across various fields. The future directions include using the suggested method on more different kinds of microstrip antennas and combining it with ensemble models to improve predictions of antenna design parameters.

Acknowledgement: We thank Vellore Institute of Technology for supporting us with the APC.

Funding Statement: This research received no external funding.

Author Contributions: Investigation, software, writing, original draft preparation and validation: Sherly Alphonse. Writing-review & editing: Abinaya S. and Sourabh Paul. All authors have read and agreed to the published version of the manuscript.

Availability of Data and Materials: R. Machado, Metamaterial Antennas. 2019. [Online]. Available: <https://www.kaggle.com/datasets/renanmav/metamaterial-antennas/>.

Conflicts of Interest: The authors declare that they have no conflicts of interest to report regarding the present study.

References

- [1] N. K. Grady *et al.*, “Terahertz metamaterials for linear polarization conversion and anomalous refraction,” *Science*, vol. 340, no. 6138, pp. 1304–1307, 2013. doi: [10.1126/science.1235399](https://doi.org/10.1126/science.1235399).
- [2] J. Shabanpour, S. Beyraghi, F. Ghorbani, and H. Oraizi, “Implementation of conformal digital metasurfaces for THz polarimetric sensing,” arXiv preprint arXiv:2101.02298, 2021.
- [3] J. Shabanpour, “Full manipulation of the power intensity pattern in a large space-time digital metasurface: From arbitrary multibeam generation to harmonic beam steering scheme,” *Ann. Phys.*, vol. 532, no. 10, pp. 2000321, 2020. doi: [10.1002/andp.202000321](https://doi.org/10.1002/andp.202000321).
- [4] M. El Sayed *et al.*, “Al-biruni earth radius (BER) metaheuristic search optimization algorithm,” *Comput. Syst. Sci. Eng.*, vol. 45, no. 2, pp. 1917–1934, 2023. doi: [10.32604/csse.2023.032497](https://doi.org/10.32604/csse.2023.032497).
- [5] H. Sun, X. Chen, Q. Shi, M. Hong, X. Fu and N. D. Sidiropoulos, “Learning to optimize: Training deep neural networks for interference management,” *IEEE Trans. Signal Process.*, vol. 66, no. 20, pp. 5438–5453, 2018. doi: [10.1109/TSP.2018.2866382](https://doi.org/10.1109/TSP.2018.2866382).
- [6] M. S. Ibrahim, A. S. Zamzam, X. Fu, and N. D. Sidiropoulos, “Learning-based antenna selection for multicasting,” in *Proc. of the 2018 IEEE 19th Int. Workshop Signal Process. Adv. Wirel. Commun. (SPAWC)*, Kalamata, Greece, 2018, pp. 25–28.
- [7] A. M. Elbir and K. V. Mishra, “Joint antenna selection and hybrid beamformer design using unquantized and quantized deep learning networks,” *IEEE Trans. Wirel. Commun.*, vol. 19, no. 3, pp. 1677–1688, 2020. doi: [10.1109/TWC.2019.2956146](https://doi.org/10.1109/TWC.2019.2956146).
- [8] J. Joung, “Machine learning-based antenna selection in wireless communications,” *IEEE Commun. Lett.*, vol. 20, no. 11, pp. 2241–2244, 2016. doi: [10.1109/LCOMM.2016.2594776](https://doi.org/10.1109/LCOMM.2016.2594776).
- [9] P. Bardalai, H. Neog, P. E. Dutta, N. Medhi, and S. K. Deka, “Throughput prediction in smart healthcare network using machine learning approaches,” in *2022 IEEE 19th India Council Int. Conf. (INDICON)*, Kochi, India, Nov 24, 2022, pp. 1–6. doi: [10.1109/INDICON56171.2022.10040160](https://doi.org/10.1109/INDICON56171.2022.10040160).
- [10] S. Ulker, “Support vector regression analysis for the design of feed in a rectangular patch antenna,” in *Proc. of the 2019 3rd Int. Symp. on Multidisp. Studies Innov. Technol. (ISMSIT)*, Ankara, Turkey, 2019, pp. 11–13.
- [11] B. Üstün, W. J. Melssen, and L. M. Buydens, “Facilitating the application of support vector regression by using a universal Pearson VII function based kernel,” *Chemom. Intell. Lab. Syst.*, vol. 81, no. 1, pp. 29–40, 2006. doi: [10.1016/j.chemolab.2005.09.003](https://doi.org/10.1016/j.chemolab.2005.09.003).
- [12] P. Mahouti, A. Belen, O. Tari, M. A. Belen, S. Karahan and S. Koziel, “Data-driven surrogate-assisted optimization of metamaterial-based filtenna using deep learning,” *Electronics*, vol. 12, no. 7, pp. 1584, 2023. doi: [10.3390/electronics12071584](https://doi.org/10.3390/electronics12071584).

- [13] A. Pietrenko-Dabrowska and S. Koziel, "Rapid antenna optimization with restricted sensitivity updates by automated dominant direction identification," *Knowl.-Based Syst.*, vol. 268, no. 2, pp. 110453, 2023. doi: [10.1016/j.knsys.2023.110453](https://doi.org/10.1016/j.knsys.2023.110453).
- [14] S. Koziel and A. Pietrenko-Dabrowska, "Improved-Efficacy EM-driven optimization of antenna structures using adaptive design specifications and variable-resolution models," *IEEE Trans. Antennas Propag.*, vol. 71, no. 2, pp. 1863–1874, 2023. doi: [10.1109/TAP.2023.3234167](https://doi.org/10.1109/TAP.2023.3234167).
- [15] S. Koziel, M. A. Belen, A. Çali,skan, and P. Mahouti, "Rapid design of 3D reflectarray antennas by inverse surrogate modeling and regularization," *IEEE Access*, vol. 11, pp. 24175–24184, 2023. doi: [10.1109/ACCESS.2023.3254204](https://doi.org/10.1109/ACCESS.2023.3254204).
- [16] N. Calik, F. Güne, S. Koziel, A. Pietrenko-Dabrowska, M. A. Belen and P. Mahouti, "Deep-learning-based precise characterization of microwave transistors using fully-automated regression surrogates," *Sci. Rep.*, vol. 13, no. 1, pp. 1445, 2023. doi: [10.1038/s41598-023-28639-4](https://doi.org/10.1038/s41598-023-28639-4).
- [17] S. Koziel, A. Pietrenko-Dabrowska, and A. G. Raef, "Knowledge-based expedited parameter tuning of microwave passives by means of design requirement management and variable-resolution EM simulations," *Sci. Rep.*, vol. 13, no. 1, pp. 334, 2023. doi: [10.1038/s41598-023-27532-4](https://doi.org/10.1038/s41598-023-27532-4).
- [18] S. Mirjalili, S. M. Mirjalili, and A. Lewis, "Grey wolf optimizer," *Adv. Eng. Softw.*, vol. 69, pp. 46–61, 2014. doi: [10.1016/j.advengsoft.2013.12.007](https://doi.org/10.1016/j.advengsoft.2013.12.007).
- [19] M. M. Eid, E. S. El-kenawy, and A. Ibrahim, "A binary sine cosine-modified whale optimization algorithm for feature selection," in *2021 National Computing Colleges Conference (NCCC)*, Taif, Saudi Arabia, 2021, pp. 1–6. doi: [10.1109/NCCC49330.2021.9428794](https://doi.org/10.1109/NCCC49330.2021.9428794).
- [20] R. Bello, Y. Gomez, A. Nowe, and M. M. Garcia, "Two-step particle swarm optimization to solve the feature selection problem," in *Seventh Int. Conf. Intell. Syst. Design Appl. (ISDA 2007)*, Rio de Janeiro, Brazil, 2007, pp. 691–696. doi: [10.1109/ISDA.2007.101](https://doi.org/10.1109/ISDA.2007.101).
- [21] H. M. Mohammed, S. U. Umar, and T. A. Rashid, "A systematic and meta-analysis survey of whale optimization algorithm," *Comput. Intell. Neurosci.*, vol. 2019, no. 1, pp. 1–25, 2019. doi: [10.1155/2019/8718571](https://doi.org/10.1155/2019/8718571).
- [22] J. H. Holland, "Genetic algorithms," *Sci. Am.*, vol. 267, no. 1, pp. 66–73, 1992. doi: [10.1038/scientificamerican0792-66](https://doi.org/10.1038/scientificamerican0792-66).
- [23] R. Storn and K. Price, "Differential evolution_A simple and efficient heuristic for global optimization over continuous spaces," *J. Glob. Optim.*, vol. 11, no. 4, pp. 341–359, 1997. doi: [10.1023/A:1008202821328](https://doi.org/10.1023/A:1008202821328).
- [24] A. Pietrenko-Dabrowska, S. Koziel, and L. Golunski, "Two-stage variable-fidelity modeling of antennas with domain confinement," *Sci. Rep.*, vol. 12, no. 1, pp. 17275, 2022. doi: [10.1038/s41598-022-20495-y](https://doi.org/10.1038/s41598-022-20495-y).
- [25] M. H. Jwair and T. A. Elwi, "Metasurface antenna circuitry for 5G communication networks," *Infocommunications J.*, vol. 15, no. 2, pp. 2–7, 2023. doi: [10.36244/ICJ.2023.2.1](https://doi.org/10.36244/ICJ.2023.2.1).
- [26] R. Machado, "Metamaterial antennas," 2019. Accessed: Jun. 06, 2023. [Online]. Available: <https://www.kaggle.com/datasets/renanmav/metamaterial-antennas>.
- [27] N. Boumal, B. Mishra, P. A. Absil, and R. Sepulchre, "Manopt, a Matlab toolbox for optimization on manifolds," *J. Mach. Learn. Res.*, vol. 15, no. 1, pp. 1455–1459, 2014.
- [28] A. Maćkiewicz and W. Ratajczak, "Principal components analysis (PCA)," *Comput. Geosci.*, vol. 19, no. 3, pp. 303–342, 1993. doi: [10.1016/0098-3004\(93\)90090-R](https://doi.org/10.1016/0098-3004(93)90090-R).
- [29] Z. Wang, X. Xiao, Y. Pang, and W. Su, "Non-invasive, intelligent, and continuous monitoring of human blood glucose with UWB dual-antenna and cascade CNN," *Meas. Sci. Technol.*, vol. 34, no. 9, pp. 095702, 2023. doi: [10.1088/1361-6501/acd138](https://doi.org/10.1088/1361-6501/acd138).
- [30] J. Bi, H. Yuan, J. Zhai, M. Zhou, and H. V. Poor, "Self-adaptive bat algorithm with genetic operations," *IEEE/CAA J. Autom. Sin.*, vol. 9, no. 7, pp. 1284–1294, 2022. doi: [10.1109/JAS.2022.105695](https://doi.org/10.1109/JAS.2022.105695).
- [31] D. Khafaga *et al.*, "Improved prediction of metamaterial antenna bandwidth using adaptive optimization of LSTM," *Comput. Mater. Contin.*, vol. 73, no. 1, pp. 865–881, 2022. doi: [10.32604/cmc.2022.028550](https://doi.org/10.32604/cmc.2022.028550).
- [32] J. Lan, X. Bu, Y. Meng, and Y. Li, "Sound insulation mechanism and prediction of membrane-type acoustic metamaterial with multi-state anti-resonances by weighted-kNN," *Appl. Phys. Express*, vol. 16, no. 8, pp. 085501, 2023. doi: [10.35848/1882-0786/acf184](https://doi.org/10.35848/1882-0786/acf184).

- [33] H. Wen, J. Yu, G. Pan, X. Chen, S. Zhang and S. Xu, “A hybrid CNN-LSTM architecture for high accurate edge-assisted bandwidth prediction,” *IEEE Wireless Commun. Lett.*, vol. 11, no. 12, pp. 2640–2644, 2022. doi: [10.1109/LWC.2022.3213017](https://doi.org/10.1109/LWC.2022.3213017).
- [34] A. Ibrahim, H. Abutarboush, A. Mohamed, M. Fouad, and E. El-Kenawy, “An optimized ensemble model for prediction the bandwidth of metamaterial antenna,” *Comput. Mater. Contin.*, vol. 71, no. 1, pp. 199–213, 2022. doi: [10.32604/cmc.2022.021886](https://doi.org/10.32604/cmc.2022.021886).
- [35] N. Kurniawati, D. N. Putri, and Y. K. Ningsih, “Random forest regression for predicting metamaterial antenna parameters,” in *2020 2nd Int. Conf. on Ind. Electr. Electron. (ICIEE)*, Lombok, Indonesia, 2020, pp. 174–178. doi: [10.1109/ICIEE49813.2020.9276899](https://doi.org/10.1109/ICIEE49813.2020.9276899).
- [36] R. W. Ziolkowski, P. Jin, and C. C. Lin, “Metamaterial-inspired engineering of antennas,” in *Proc. IEEE*, vol. 99, no. 10, pp. 1720–1731, 2010. doi: [10.1109/JPROC.2010.2091610](https://doi.org/10.1109/JPROC.2010.2091610).
- [37] A. A. Abdelhamid and S. R. Alotaibi, “Optimized two-level ensemble model for predicting the parameters of metamaterial antenna,” *Comput. Mater. Contin.*, vol. 73, no. 1, pp. 917–933, 2022. doi: [10.32604/cmc.2022.027653](https://doi.org/10.32604/cmc.2022.027653).
- [38] A. H. Alharbi *et al.*, “Improved dipper-throated optimization for forecasting metamaterial design bandwidth for engineering applications,” *Biomimetics*, vol. 8, no. 2, pp. 241, 2023. doi: [10.3390/biomimetics8020241](https://doi.org/10.3390/biomimetics8020241).
- [39] M. Yadav, G. S. Chandel, and R. Gupta, “Review of image classification techniques based on LDA, PCA and genetic algorithm,” *Int. J. Eng. Sci. Res. Technol.*, vol. 3, no. 2, 2014. Accessed: Jun. 23, 2023. [Online]. Available: <https://europub.co.uk/articles/nbspreview-of-image-classification-techniques-based-on-lda-pca-and-genetic-algorithm-A-100880>